



Original scientific paper

## Improving hot corrosion behaviour of Cr<sub>3</sub>C<sub>2</sub>-25NiCr coatings by reinforcing nano yttria-stabilized zirconia at 850 °C

Sukhjinder Singh<sup>1</sup>, Khushdeep Goyal<sup>1,✉</sup> and Rakesh Bhatia<sup>2</sup>

<sup>1</sup>Department of Mechanical Engineering, Punjabi University, Patiala, India

<sup>2</sup>Yadavindra Department of Engineering, Punjabi University Guru Kashi Campus, Damdama Sahib, India

Corresponding authors: ✉ [khushgoyal@yahoo.com](mailto:khushgoyal@yahoo.com); tel.: +20502327236

Received: August 27, 2024; Accepted: October 5, 2024; Published: October 7, 2024

### Abstract

High-temperature corrosion poses a significant threat to the longevity and performance of boiler tube materials in harsh industrial environments, necessitating the development of advanced protective coatings. Yttria-stabilized zirconia (YSZ)-enhanced Cr<sub>3</sub>C<sub>2</sub>-25NiCr coatings were applied to T22 boiler tube steel using the high-velocity oxyfuel method. Conventional Ni-20Cr, 5 wt.% YSZ- Cr<sub>3</sub>C<sub>2</sub>-25NiCr and 10 wt.% YSZ- Cr<sub>3</sub>C<sub>2</sub>-25NiCr composite coatings were prepared. High-temperature corrosion tests were conducted on both uncoated and coated samples in a Na<sub>2</sub>SO<sub>4</sub>-60 % V<sub>2</sub>O<sub>5</sub> environment at 850 °C under fluctuating thermal conditions. These experiments were carried out in a silicon tube furnace at high temperatures, with each sample subjected to 50 exposure cycles. Each cycle consisted of 1 h in the corrosive environment followed by 20 minutes of cooling at room temperature. Corrosion products were analysed using energy-dispersive x-ray analysis and scanning electron microscopy. The addition of YSZ to the Cr<sub>3</sub>C<sub>2</sub>-25NiCr coatings significantly improved corrosion resistance, with the Ni-20Cr, 5 wt.% YSZ-Ni-20Cr and 10 wt.% Cr<sub>3</sub>C<sub>2</sub>-25NiCr coatings reducing overall weight gain by 73.08, 84.70 and 89.96 %, respectively, compared to uncoated T22 steel.

### Keywords

Boiler steel tube; thermally sprayed coatings; zirconia ceramic; hardness

### Introduction

Material conservation is becoming increasingly vital due to the demands of the global economy, both now and in the future [1,2]. In many applications involving high-temperature aggressive environments, such as boilers, internal combustion engines, gas turbines, and industrial waste incinerators, the degradation of metals and alloys from hot corrosion and erosion poses a significant challenge [2]. This degradation ultimately leads to expensive and complex repair efforts. Consequently, any method

that can extend component lifespan is highly desirable for engineers and offers substantial financial savings. Corrosion remains a prevalent issue in various industrial applications and products, leading to the degradation and failure of components and systems. In addition to indirect costs from downtime and lost productivity, billions are spent annually replacing corroded equipment [3-5]. Premature failure of these components can also result in accidents or fatalities. In the U.S. and European Union, the direct cost of corrosion is estimated to be between three and five percent of their GDPs [5-7]. It is reported in the literature that hot corrosion and erosion account for over 50 % of boiler tube failures in thermal power plants [8]. Coal combustion produces highly corrosive compounds that deposit on boiler tubes. Sulphur and oxygen combine to form SO<sub>2</sub>, which oxidizes into SO<sub>3</sub>. SO<sub>3</sub> reacts with water vapor and NaCl to produce Na<sub>2</sub>SO<sub>4</sub>. When fuel containing vanadium is heated beyond its melting point of 550 °C, it oxidizes to form V<sub>2</sub>O<sub>5</sub>, which reacts with Na<sub>2</sub>SO<sub>4</sub> to create sodium vanadates, highly corrosive compounds with low melting points [7-10].

Thermal spraying protective coatings have proven effective without altering the base material's other properties [11]. Thermal spraying, a widely used hardfacing process, is distinct in its ability to minimize substrate dissolution, reduce heat input, and offer flexibility in material choice. While early thermally sprayed coatings had limited value for corrosion protection due to interconnected porosity, the advent of the high-velocity oxyfuel spray (HVOF) technique has led to coatings with improved corrosion resistance. HVOF coatings are dense, uniform, and sufficiently thick to block electrolyte penetration [12-14]. The low flame temperature prevents coating decomposition, while the hypersonic velocity accelerates powder and flame interaction. The continuous nature of the HVOF process also makes it more convenient to apply coatings on-site in industrial settings [12-15].

In recent years, various researchers have developed coatings using thermal spraying to enhance the properties of boiler steels. However, the porous nature of these coatings, with microcracks and voids, allows corrosive chemicals to attack the substrate steels. Thus, there remains potential for improving the mechanical and microstructural properties of these coatings. Although many studies have focused on developing Cr<sub>3</sub>C<sub>2</sub>-25NiCr coatings on steel alloys, research on nano yttria-stabilized zirconia (YSZ) reinforced composite coatings remains limited. Hence, there is significant scope for developing new nano YSZ mixed Cr<sub>3</sub>C<sub>2</sub>-25NiCr nanocomposite coatings and exploring their microstructure, porosity, and microhardness on boiler tube steels.

## Experimental

### *Development of coatings*

For the production of various coatings, commercially available Cr<sub>3</sub>C<sub>2</sub>-25NiCr powder was mixed with 5 and 10 wt.% YSZ powder using a low-energy ball milling process. To create the composite mixture, 950 g of Cr<sub>3</sub>C<sub>2</sub>-25NiCr powder was combined with 50 g of YSZ (Y<sub>2</sub>O<sub>3</sub>/ZrO<sub>2</sub>) powder, while another batch was prepared by mixing 900g of Ni-20Cr powder with 100 g of YSZ powder. The mixtures were continuously rolled at 200 rpm for 4 hours. Boiler tubes, obtained from the Guru Gobind Singh Thermal Power Plant in Ropar, India, were cut into T22 steel substrates with dimensions of 22×15×5 mm. After polishing the T22 substrates using SiC paper, they were subjected to alumina powder blasting with grit size 45. The coatings were applied using HVOF spraying equipment at Metallizing Equipment Co. Pvt. Ltd. in Jodhpur, India. The effect of YSZ addition on the microstructure of these coatings and their mechanical behaviour was evaluated by the same authors and that research has already been published [11].

### Hot corrosion investigations

Both coated and uncoated specimens were subjected to 850 °C in a silicon tube furnace, with the temperature maintained at an average of approximately 850 °C, fluctuating by  $\pm 5$  °C. Each cycle involved heating the specimens for 1 hour, followed by a 20-minute cooling period under ambient conditions. After each cycle, the surface texture of the specimens was visually inspected. Following visual examination, the specimens were cleaned with acetone, and their weights were measured using an electronic balance (CB-120, Contech Instruments Ltd., with an accuracy of 0.001 g). After completing 50 cycles, the resulting specimens were evaluated through visual examination, weight change analysis, as well as SEM/EDAX and XRD analyses.

## Results

### Visual examination

The macrographs presented in Figure 1 depict T22 steel specimens, both uncoated and coated with  $\text{Cr}_3\text{C}_2$ -25NiCr, as well as nano YSZ reinforced  $\text{Cr}_3\text{C}_2$ -25NiCr, after being exposed to 850 °C in a molten salt environment ( $\text{Na}_2\text{SO}_4$  -60 %  $\text{V}_2\text{O}_5$ ) within a silicon tube furnace. Scale formation initiated after the second cycle and continued to develop throughout the subsequent cycles. The scale, which was thick and glossy, began to crack after the 25th cycle. By the end of 50 cycles, the specimen had turned a dark blackish grey. Figure 1(a) shows that the multilayered scale, which overlapped and peeled from the top layer, appeared to be extremely thick, porous, and non-protective. Figure 1(b) displays the macrograph of a conventional  $\text{Cr}_3\text{C}_2$ -25NiCr coated specimen following hot corrosion exposure. The specimen's colour changed to yellowish grey after the 8th cycle, and minor scale swelling was observed by the end of 39 cycles. The macrographs of the 5 and 10 wt.% YSZ reinforced  $\text{Cr}_3\text{C}_2$ -25NiCr coated specimens are shown in Figures 1(c) and 1(d). Both YSZ-reinforced coatings remained intact and smooth, with no cracks or thermal spallation observed.

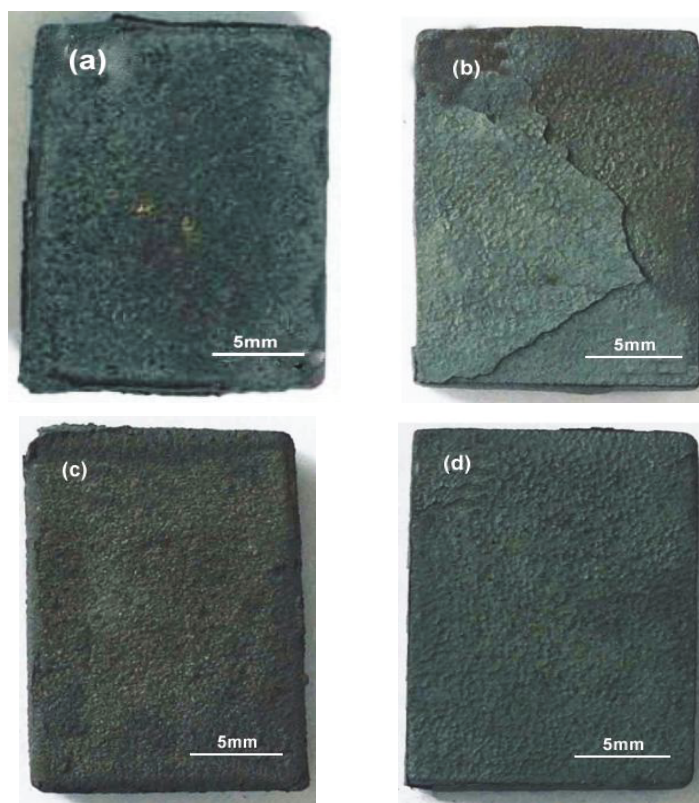


**Figure 1.** Macrographs of (a) uncoated; (b)  $\text{Cr}_3\text{C}_2$ -25NiCr; (c) 5 wt.% YSZ-  $\text{Cr}_3\text{C}_2$ -25NiCr and (d) 10wt.% YSZ- $\text{Cr}_3\text{C}_2$ -25NiCr coated T22 specimens after hot corrosion at 850 °C

Weight change data

The weight change plots for uncoated and all coated specimens after 50 cycles of hot corrosion exposure at 850 °C in a molten salt environment (Na<sub>2</sub>SO<sub>4</sub> -60 % V<sub>2</sub>O<sub>5</sub>) are shown in Figure 2. These plots were used to analyze the hot corrosion kinetics after each cycle by measuring weight gain, where a higher weight gain indicates a higher corrosion rate. For the uncoated T22 sample at 850 °C, the mass gain rate was relatively low until the 7th cycle but increased significantly after the 32<sup>nd</sup> cycle, with a cumulative weight gain of 286.17 mg cm<sup>-2</sup>. In the case of the conventional Cr<sub>3</sub>C<sub>2</sub>-25NiCr coated specimen, the plot shows an increase in weight gain starting from the 23rd cycle and continuing through to the 50<sup>th</sup> cycle, as illustrated in Figure 2. Both YSZ-reinforced Cr<sub>3</sub>C<sub>2</sub>-25NiCr coated samples showed less weight gain compared to the conventional Cr<sub>3</sub>C<sub>2</sub>-25NiCr coated specimen. The weight gain decreased with a higher weight percentage of YSZ nanoparticles in the Cr<sub>3</sub>C<sub>2</sub>-25NiCr coating. The cumulative weight gain for the Cr<sub>3</sub>C<sub>2</sub>-25NiCr coated specimen (Fig. 3) was 77.02 mg cm<sup>-2</sup>, which is significantly lower than that of the uncoated T22 steel (286.17 mg cm<sup>-2</sup>). The Cr<sub>3</sub>C<sub>2</sub>-25NiCr coating reduced the cumulative weight gain of the uncoated steel by 73.08 %. For the 5 and 10 wt.% YSZ-Cr<sub>3</sub>C<sub>2</sub>-25NiCr coated T22 specimens, the mass gain rates were 43.78 and 28.74 mg cm<sup>-2</sup>, respectively. The addition of 5 and 10 wt.% YSZ to the Cr<sub>3</sub>C<sub>2</sub>-25NiCr coating reduced the cumulative weight gain of uncoated steel by 84.70 and 89.96 %, respectively.

Figure 4 illustrates the relationship between (weight gain/area)<sup>2</sup> and the number of cycles (50 cycles), highlighting the behaviour of high-temperature corrosion at 850 °C for both uncoated and coated T22 specimens. The conventional Cr<sub>3</sub>C<sub>2</sub>-25NiCr and YSZ-reinforced Cr<sub>3</sub>C<sub>2</sub>-25NiCr coated specimens followed a nearly perfect parabolic rate law, while the uncoated T22 specimen deviated slightly from this pattern. The parabolic rate constant (K<sub>p</sub>) was calculated using the slope of the fitted linear regression line. Table 1 presents the cumulative mass gain and K<sub>p</sub> values for the specimens after hot corrosion exposure at 850 °C, revealing that all coated specimens had significantly lower K<sub>p</sub> values than the uncoated T22 steel specimen.

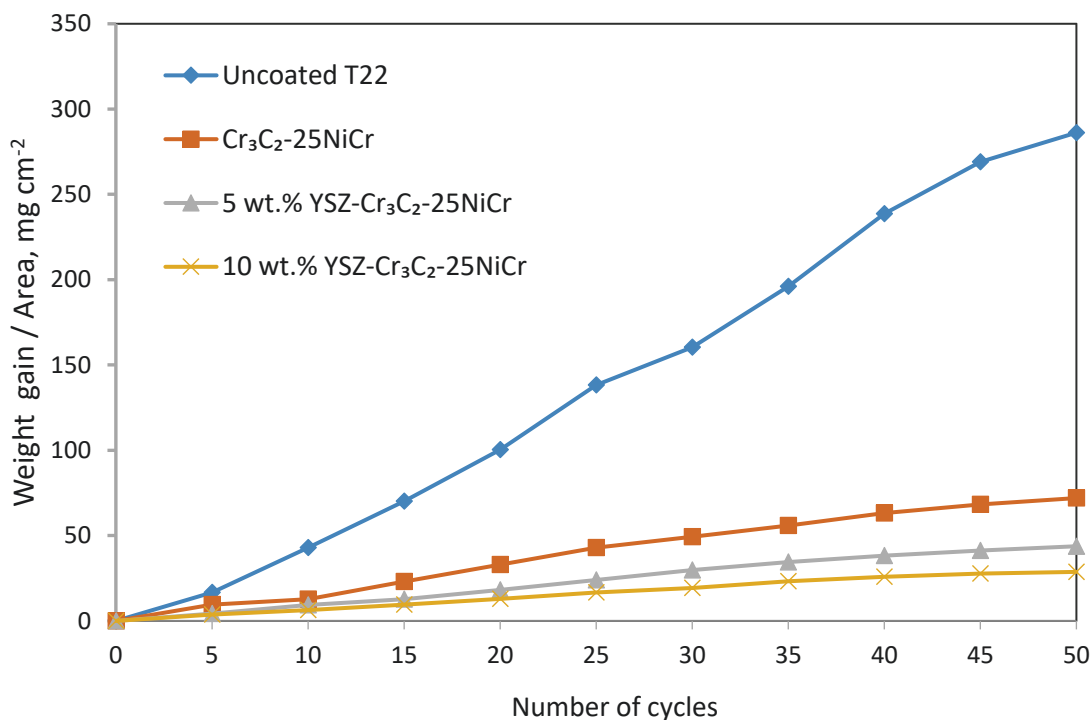


Figure 2. Weight gain/area versus time for all the specimens after hot corrosion at 850 °C

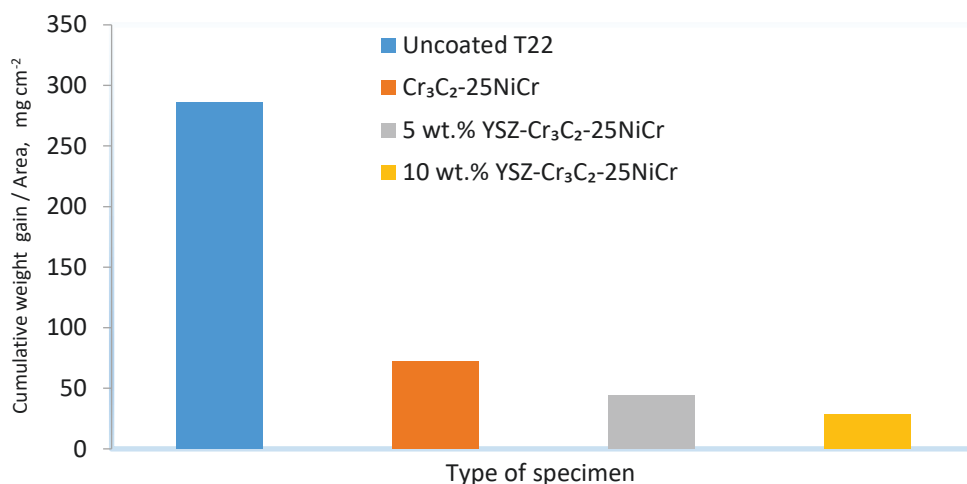


Figure 3. Cumulative weight gain for all specimens after hot corrosion at 850 °C

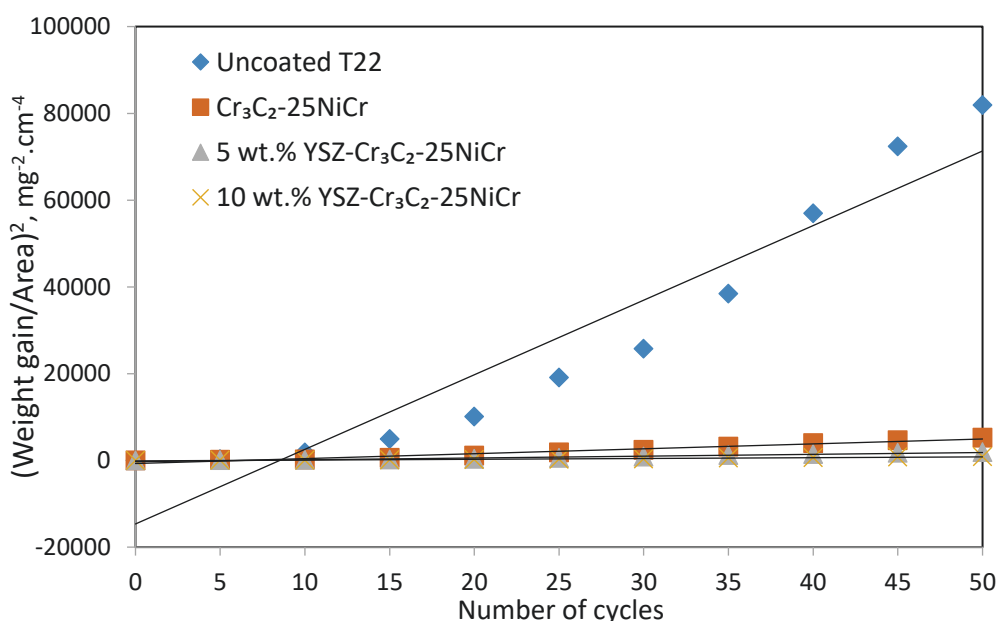


Figure 4. (Weight gain/area)<sup>2</sup> versus the number of cycles for all specimens after exposure to hot corrosion 850 °C

Table 1. Parabolic rate constant and cumulative weight gain for all specimens after hot corrosion at 850 °C in molten salt (Na<sub>2</sub>SO<sub>4</sub>- 60 % V<sub>2</sub>O<sub>5</sub>) environment

Type of coating	$K_p / 10^{-10} \text{ g}^2 \text{ cm}^{-4} \text{ s}^{-1}$	Total weight gain, $\text{mg cm}^{-2}$
Uncoated T22 steel	4549.62	286.17
Cr <sub>3</sub> C <sub>2</sub> -25NiCr	288.16	72.02
5 wt.% YSZ- (Cr <sub>3</sub> C <sub>2</sub> -25NiCr )	106.48	43.78
10 wt.% YSZ- (Cr <sub>3</sub> C <sub>2</sub> -25NiCr)	45.89	28.74

FE-SEM/energy dispersive X-ray spectroscopy analysis

The FE-SEM micrographs, along with EDAX compositional analysis, of uncoated T22 boiler steel, Cr<sub>3</sub>C<sub>2</sub>-25NiCr, 5 wt.% YSZ- Cr<sub>3</sub>C<sub>2</sub>-25NiCr and 10 wt.% YSZ- Cr<sub>3</sub>C<sub>2</sub>-25NiCr coated specimens after 50 cycles of hot corrosion at 850 °C in a molten salt environment (Na<sub>2</sub>SO<sub>4</sub> -60 % V<sub>2</sub>O<sub>5</sub>) are displayed in Figure 5. The oxide scale formed on the uncoated T22 steel specimen was found to be porous, with

a nodular structure and surface cracks, as shown in Figure 5(a). SEM analysis indicated that the scale was non-protective and susceptible to corrosion.

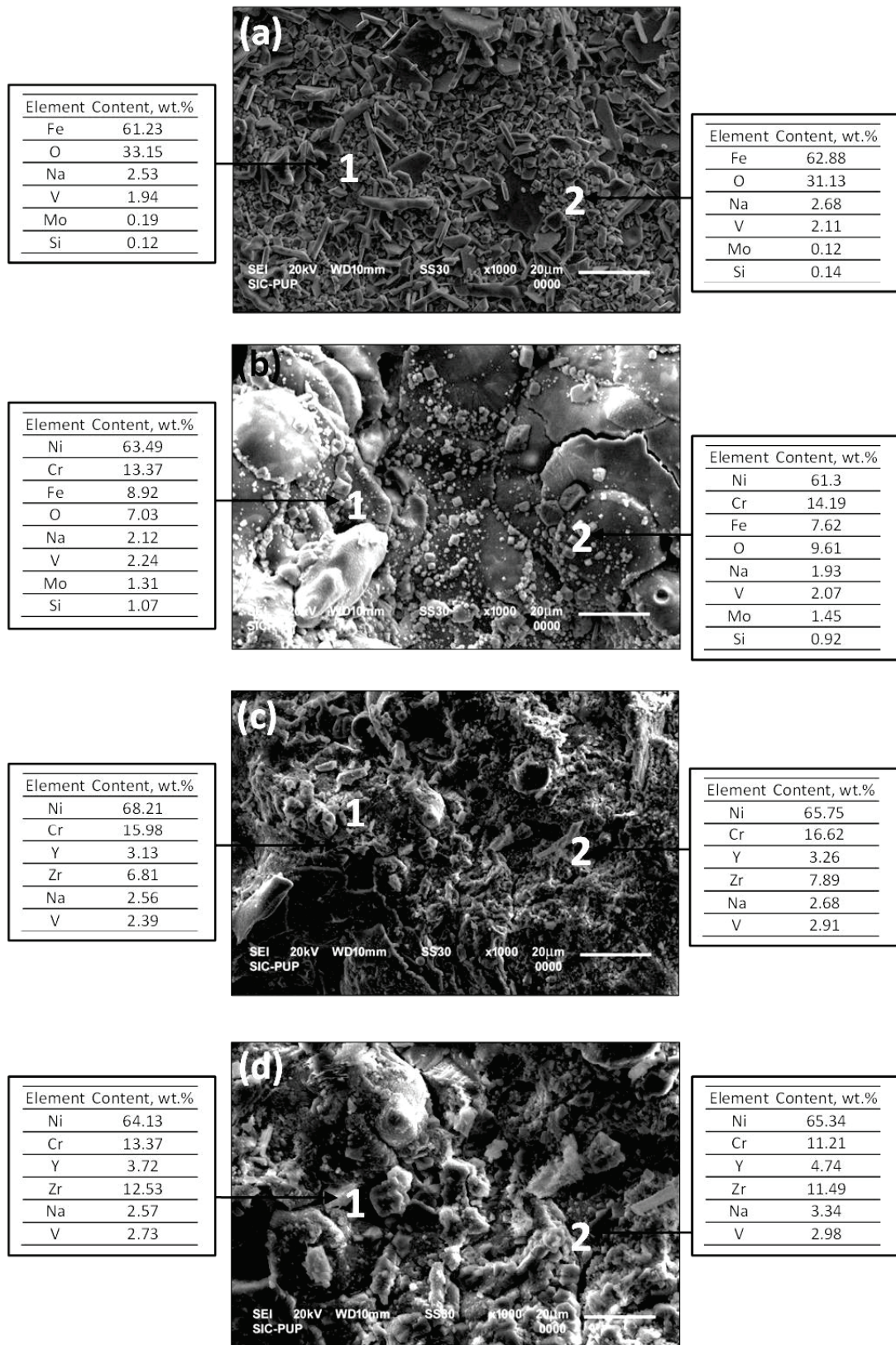


**Figure 5.** SEM/EDAX analysis of (a) un-coated (b) Cr<sub>3</sub>C<sub>2</sub>-25NiCr (c) 5wt.% YSZ- Cr<sub>3</sub>C<sub>2</sub>-25NiCr and (d) 10 wt.% YSZ- Cr<sub>3</sub>C<sub>2</sub>-25NiCr coated T22 steel samples after hot corrosion at 850 °C

EDAX compositional analysis revealed significant amounts of Na and V, along with high concentrations of Fe and O, at specific observation points. Minor amounts of Mo and Si were also detected.

The EDAX analysis suggested the possible formation of Fe, Na, V, and Mo oxides in the scale, with Fe being the predominant element.

The micrograph of the conventional  $\text{Cr}_3\text{C}_2$ -25NiCr coated T22 specimen after hot corrosion exposure, shown in Figure 5 (b), revealed white-greyish phases, with EDAX analysis at points 1 and 2 indicating a high content of Ni, Cr, C and along with minor amounts of Fe, Mo, O, Na, and V. The diffusion of Fe and Mo from the substrate during hot corrosion exposure might be attributed to the porous nature of the conventional  $\text{Cr}_3\text{C}_2$ -25NiCr coating. The presence of Fe and O indicated the formation of  $\text{Fe}_2\text{O}_3$ . The micrographs of the 5 wt.% YSZ-Ni-20Cr and 10 wt.% YSZ-  $\text{Cr}_3\text{C}_2$ -25NiCr coated T22 steel specimens, shown in Figure 5 (c) and Figure 5 (d), revealed substantial amounts of Ni and Cr, along with minor elements such as C, Y, Zr, Na, and V in the scale composition. The presence of Zr and Y confirmed the incorporation of YSZ nanoparticles in the oxide scale. The scales on these specimens appeared uniform, with regular morphology, and remained intact. The minor presence of Na and V in the EDAX analysis at selected points after hot corrosion at 850 °C further confirmed the presence of molten salt elements during the experiment.

#### X-ray diffraction analysis

The X-ray diffraction analysis of uncoated T22 boiler steel,  $\text{Cr}_3\text{C}_2$ -25NiCr, 5 wt.% YSZ- $\text{Cr}_3\text{C}_2$ -25NiCr, and 10 wt.% YSZ- $\text{Cr}_3\text{C}_2$ -25NiCr coated specimens after hot corrosion exposure at 850 °C in a molten salt environment is presented in Figure 6 (a)–(d). In the corroded uncoated T22 specimen, the scale revealed major peaks of  $\text{Fe}_2\text{O}_3$  along with  $\text{Cr}_3\text{C}_2$ , as shown in Figure 6(a).

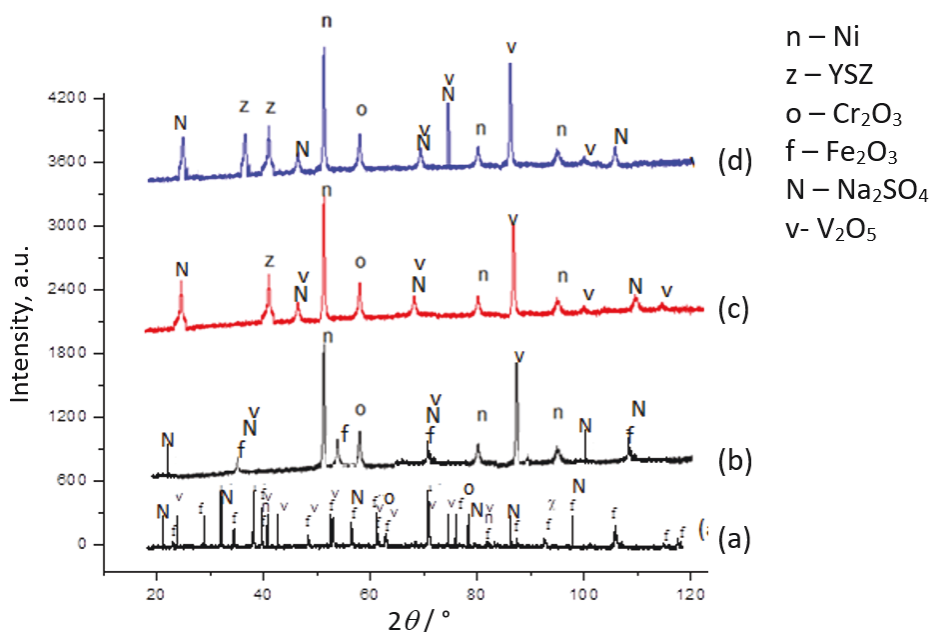


**Figure 6.** XRD graph of (a) uncoated; (b)  $\text{Cr}_3\text{C}_2$ -25NiCr; (c) 5wt.% YSZ-  $\text{Cr}_3\text{C}_2$ -25NiCr; and (d) 10 wt.% YSZ-  $\text{Cr}_3\text{C}_2$ -25NiCr coated T22 specimens after hot corrosion at 850 °C

Small peaks of  $\text{Fe}_2\text{O}_3$ ,  $\text{Cr}_3\text{C}_2$  and  $\text{Cr}_2\text{O}_3$  were detected on the conventional  $\text{Cr}_3\text{C}_2$ -25NiCr coated T22 steel specimen, likely due to the diffusion of Fe from the substrate towards the coating surface, a phenomenon that may be attributed to the porous nature of the coating. XRD analysis of the 5 wt.% YSZ-  $\text{Cr}_3\text{C}_2$ -25NiCr and 10 wt.% YSZ-  $\text{Cr}_3\text{C}_2$ -25NiCr coated specimens after hot corrosion exposure revealed peaks of Ni,  $\text{Cr}_2\text{O}_3$ ,  $\text{Cr}_3\text{C}_2$  and  $\text{ZrO}_2$ - $\text{Y}_2\text{O}_3$  (YSZ), as shown in Figure 6(c) and Figure 6(d). Additionally, minor peaks of  $\text{Na}_2\text{SO}_4$  and  $\text{V}_2\text{O}_5$  were observed in all specimens after corrosion at 850 °C in the molten salt environment, as indicated in Figures 6 (a) to 6(d), confirming the presence of sulphates and vanadates in the molten salt.

## Discussion

In a Na<sub>2</sub>SO<sub>4</sub>-60 % V<sub>2</sub>O<sub>5</sub> atmosphere at 850 °C for 50 cycles, the uncoated T22 steel experienced severe corrosion. Figure 2 presents the plot of cumulative weight gain over time for the steel specimen. The weight gain followed a parabolic trend with only minor fluctuations. For the uncoated T22 steel, the weight change plot indicates a consistent increase in weight throughout the experiment. The difference in the parabolic rate constant ( $K_p$ ) between coated and uncoated steel specimens at 850 °C is due to the higher rate of weight gain observed in the uncoated specimens compared to the coated ones. The formation of Fe<sub>2</sub>O<sub>3</sub> in the spalled scale was reported, and it was confirmed that it was non-protective during hot corrosion studies on iron aluminide alloys in a Na<sub>2</sub>SO<sub>4</sub> atmosphere [16-18]. After the second cycle of hot corrosion exposure, significant thermal spalling of the oxide scale was observed in the uncoated T22 steel. By the final exposure cycle, the scale had completely detached from the substrate. Similar phenomena of spallation and scale detachment were also studied by Goyal *et al.* [19] and Sidhu *et al.* [20]. For the uncoated T22 specimen, the  $K_p$  values were  $4549.62 \times 10^{-10} \text{ g}^2 \text{ cm}^{-4} \text{ s}^{-1}$ , and the total mass gain after the completion of 50 cycles was observed as  $286.17 \text{ mg cm}^{-2}$ . The substantial increase in weight during the study is likely due to the rapid uptake of oxygen through diffusion, consistent with findings reported in the literature [22,23]. Hot corrosion of T22 steel in a molten salt environment at 850 °C led to the formation of a non-protective Fe<sub>2</sub>O<sub>3</sub> scale after 50 cycles on the bare specimens. XRD analysis of the Cr<sub>3</sub>C<sub>2</sub>-25NiCr-coated boiler steel after oxidation in a Na<sub>2</sub>SO<sub>4</sub>-60 % V<sub>2</sub>O<sub>5</sub> environment at 850 °C revealed that Ni and Cr<sub>2</sub>O<sub>3</sub> were the primary phases in the oxide scale, with Fe<sub>2</sub>O<sub>3</sub> also present, as shown in Figure 6. XRD, SEM/EDAX, and X-ray mapping analyses confirmed the presence of Fe and O in the scale, verifying the formation of a non-protective Fe<sub>2</sub>O<sub>3</sub> layer. Additionally, SEM/EDAX and X-ray mapping revealed the presence of Mo in the coating scale, suggesting the formation of Mo oxide.

The weight gain data for Cr<sub>3</sub>C<sub>2</sub>-25NiCr-coated T22 boiler tube steel demonstrated that the Cr<sub>3</sub>C<sub>2</sub>-25NiCr coating effectively reduced weight gain compared to uncoated T22 steel after exposure to hot corrosion in a Na<sub>2</sub>SO<sub>4</sub>-60 % V<sub>2</sub>O<sub>5</sub> environment at 850 °C (see Figures 2 and 3). The Cr<sub>3</sub>C<sub>2</sub>-25NiCr-coated specimen exhibited a cumulative weight gain of  $77.02 \text{ mg cm}^{-2}$ , considerably lower than the  $286.17 \text{ mg cm}^{-2}$  observed for the uncoated T22 steel. The coating achieved a 73.08 % reduction in cumulative weight gain compared to the uncoated steel. The weight gain of the Cr<sub>3</sub>C<sub>2</sub>-25NiCr-coated T22 boiler steel displayed a parabolic trend with only minor deviations. The deviation from the parabolic behaviour may be due to inhomogeneous oxides as explained by Goyal *et al.* [19] and Sidhu *et al.* [20]. The weight gain rate of the Cr<sub>3</sub>C<sub>2</sub>-25NiCr-coated specimen initially increased but decreased towards the end of the study, likely due to the formation of oxides at the splat boundaries. Similar results have been reported in the literature by various authors [19-22]. The formation and dissolution of Cr<sub>2</sub>O<sub>3</sub> occurred simultaneously, a process known as basic fluxing. Due to molten salts, Cr<sub>2</sub>O<sub>3</sub> dissolved into ions and then reprecipitated from the molten salts as flaky Cr<sub>2</sub>O<sub>3</sub> structures [10,12]. SEM/EDS analysis confirmed these results. The coating demonstrated superior corrosion resistance compared to uncoated steel, attributed to the significantly flattened splats, which increased the distance between the coating surface and the coating/substrate interface along the splat boundary [12].

The T22 boiler steel specimens coated with 5 wt.% YSZ- Cr<sub>3</sub>C<sub>2</sub>-25NiCr and 10 wt.% YSZ- Cr<sub>3</sub>C<sub>2</sub>-25NiCr showed lower weight gain after hot corrosion in a Na<sub>2</sub>SO<sub>4</sub>-60 % V<sub>2</sub>O<sub>5</sub> environment at 850 °C compared to the uncoated and Cr<sub>3</sub>C<sub>2</sub>-25NiCr-coated T22 steel. The mass gain rates for the 5 wt.% and 10 wt.% YSZ- Cr<sub>3</sub>C<sub>2</sub>-25NiCr-coated specimens were  $43.78$  and  $28.74 \text{ mg cm}^{-2}$ , respectively. Adding 5 and 10 wt.% YSZ to the Cr<sub>3</sub>C<sub>2</sub>-25NiCr coating reduced the cumulative weight gain compared

to uncoated steel by 84.70 and 89.96 %, respectively. This indicates that increasing the YSZ content from 5 to 10 wt.% significantly reduces the corrosion rate. The improvement is likely due to the nano-sized YSZ particles filling the pores in the Cr<sub>3</sub>C<sub>2</sub>-25NiCr coating, thereby inhibiting weight gain during the study. Various studies have demonstrated that incorporating nanoparticles into conventional coatings can reduce weight gain. Goyal and Goyal [23] and Karaoglanli *et al.* [24] found that increasing the weight percentage of nanoparticles in conventional coatings reduced cumulative weight gain. This reduction is attributed to the homogeneous dispersion of nanoparticles, which enhances nanocomposite coatings' mechanical and thermal properties, thereby improving their corrosion resistance at high temperatures. XRD analysis of specimens coated with 5 wt.% YSZ- Cr<sub>3</sub>C<sub>2</sub>-25NiCr and 10 wt.% YSZ- Cr<sub>3</sub>C<sub>2</sub>-25NiCr after hot corrosion exposure showed peaks for Ni, Cr<sub>2</sub>O<sub>3</sub>, and ZrO<sub>2</sub>-Y<sub>2</sub>O<sub>3</sub>. The presence of ZrO<sub>2</sub>-Y<sub>2</sub>O<sub>3</sub> peaks confirmed the inclusion of nano YSZ particles in the Cr<sub>3</sub>C<sub>2</sub>-25NiCr coating matrix. The formation of protective layers of Ni, Cr<sub>2</sub>O<sub>3</sub>, and ZrO<sub>2</sub>-Y<sub>2</sub>O<sub>3</sub> during hot corrosion at 850 °C helped block corrosive elements, enhancing the hot corrosion resistance compared to the Cr<sub>3</sub>C<sub>2</sub>-25NiCr coating alone. The 5 wt.% YSZ- Cr<sub>3</sub>C<sub>2</sub>-25NiCr and 10 wt.% YSZ- Cr<sub>3</sub>C<sub>2</sub>-25NiCr reinforced coatings remained intact, as shown by SEM micrographs, and EDAX analysis confirmed the presence of Ni, Cr, Y, and Z at selected points (see Figure 5). Kumar *et al.* [25] reported that nanocomposite coatings exhibited improved properties when compared with coarse materials due to the unique characteristics of the nanoscale materials present in the coatings. These improvements include better mechanical properties (tensile strength, impact resistance, micro-hardness) and enhanced corrosion resistance. Coatings with higher hardness generally exhibit greater corrosion resistance than those with lower hardness. Therefore, incorporating YSZ nanoparticles into the Cr<sub>3</sub>C<sub>2</sub>-25NiCr coating significantly improved its hot corrosion resistance at 850 °C in a Na<sub>2</sub>SO<sub>4</sub>-60 % V<sub>2</sub>O<sub>5</sub> molten salt environment.

## Conclusions

This study examined the hot corrosion behaviour of bare T22 steel, Cr<sub>3</sub>C<sub>2</sub>-25NiCr -coated T22, and T22 steel coated with 5 and 10 wt.% YSZ- Cr<sub>3</sub>C<sub>2</sub>-25NiCr, all subjected to 850 °C in a molten salt environment. The findings are summarized as follows:

- After 50 cycles at 850°C in a Na<sub>2</sub>SO<sub>4</sub>-60 % V<sub>2</sub>O<sub>5</sub> atmosphere, the uncoated T22 steel displayed significant corrosion.
- The Cr<sub>3</sub>C<sub>2</sub>-25NiCr coating on the T22 steel demonstrated lower weight gain compared to the uncoated steel when exposed to hot corrosion at 850 °C.
- Over the 50-cycle test period, the Cr<sub>3</sub>C<sub>2</sub>-25NiCr, 5 wt.% YSZ- Cr<sub>3</sub>C<sub>2</sub>-25NiCr, and 10 wt.% YSZ- Cr<sub>3</sub>C<sub>2</sub>-25NiCr coatings reduced the overall weight gain rate by 73.08, 84.70 and 89.96, respectively, relative to bare T22 steel.
- The corrosion resistance of the coatings in the molten salt environment followed the order: 10 wt.% YSZ- Cr<sub>3</sub>C<sub>2</sub>-25NiCr > 5 wt.% YSZ- Cr<sub>3</sub>C<sub>2</sub>-25NiCr > Cr<sub>3</sub>C<sub>2</sub>-25NiCr.

The incorporation of nano YSZ particles reduced porosity and enhanced corrosion resistance by filling voids in the Cr<sub>3</sub>C<sub>2</sub>-25NiCr coating and forming an interlocking structure that prevents the penetration of corrosive species.

**Acknowledgements:** This research received no specific grant from any funding agency in the public, commercial, or not-for-profit sectors

**Conflicts of interest:** The authors declare that they have no conflict of interest.

## References

- [1] B. S. Sidhu S. Prakash, Erosion-corrosion of plasma as sprayed and laser remelted Stellite-6 coatings in a coal fired boiler, *Wear* **260** (2006) 1035-1044. <https://doi.org/10.1016/j.wear.2005.07.003>
- [2] H. Guo, W. Fan, Y. Liu, J. Long, Experimental investigation on the high-temperature corrosion of 12Cr1MoVG boiler steel in waste-to-energy plants: Effects of superheater operating temperature and moisture, *Process Safety and Environmental Protection* **188** (2024) 573-583. <https://doi.org/10.1016/j.psep.2024.05.130>
- [3] T. Sidhu, S. Prakash, R. Agrawal, Study of Molten Salt Corrosion of Superni-75 using Termogravimetric Technique, *Journal of Naval Architecture and Marine Engineering* **3** (2006) 77-82. <https://doi.org/10.1016/j.psep.2024.05.130>
- [4] J. Lehmusto, D. Lindberg, P. Yrjas, L. Hupa, The Effect of Temperature on the Formation of Oxide Scales Regarding Commercial Superheater Steels, *Oxidation of Metals* **89** (2018) 251-278. <https://doi.org/10.1007/s11085-017-9785-6>
- [5] T. Sidhu, S. Prakash, R. Agrawal, Hot corrosion studies of HVOF sprayed Cr<sub>3</sub>C<sub>2</sub>-NiCr and Ni-20Cr coatings on nickel-based superalloy at 900° C, *Surface and Coatings Technology* **201** (2006) 792-800. <https://doi.org/10.1016/j.surfcoat.2005.12.030>
- [6] Y. Ozgurluk, K. M. Doleker, A. C. Karaoglanli, Hot corrosion behavior of YSZ, Gd<sub>2</sub>Zr<sub>2</sub>O<sub>7</sub> and YSZ/Gd<sub>2</sub>Zr<sub>2</sub>O<sub>7</sub> thermal barrier coatings exposed to molten sulfate and vanadate salt, *Applied Surface Science* **438** (2017) 96-113. <https://doi.org/10.1016/j.apsusc.2017.09.047>
- [7] B.K. Bhagria, D. Mudgal, S.S. Sidhu, R. Verma, Present scenario of hot corrosion studies performed with ferritic steel, *AIP Conference Proceedings* **2341(1)** (2021) 040034. <https://doi.org/10.1063/5.0049955>
- [8] R. Kumar, R. Singh, S. Kumar, S., Erosion and hot corrosion phenomena in thermal power plant and their preventive methods: a study, *Asian Review of Mechanical Engineering* **7** (2018) 38-45.
- [9] K. Goyal, H. Singh, R. Bhatia, Effect of Carbon Nanotubes on Properties of Ceramics Based Composite Coatings, *Advanced Engineering Forum* **26** (2018) 53-66. <https://doi.org/10.4028/www.scientific.net/AEF.26.53>
- [10] D. K. Goyal, H. Singh, H. Kumar, V. Sahni, Slurry erosion behaviour of HVOF sprayed WC-10Co-4Cr and Al<sub>2</sub>O<sub>3</sub>+ 13TiO<sub>2</sub> coatings on a turbine steel, *Wear* **289** (2012) 46-57. <https://doi.org/10.1016/j.wear.2012.04.016>
- [11] S. Singh, K. Goyal, R. Bhatia, Mechanical and microstructural properties of yttria-stabilized zirconia reinforced Cr<sub>3</sub>C<sub>2</sub>-25NiCr thermal spray coatings on steel alloy, *Journal of Electrochemical Science and Engineering* **12(5)** (2022) 819-828. <https://doi.org/10.5599/jese.1278>
- [12] S. Singh, K. Goyal, R. Bhatia, Effect of nano yttria-stabilized zirconia on properties of Ni-20Cr composite coatings, *Journal of Electrochemical Science and Engineering* **12(5)** (2022) 901-909. <https://doi.org/10.5599/jese.1319>
- [13] M. Kuruba, G. Gaikwad, D. Shivalingappa, Hot-corrosion behaviour of CNT reinforced Cr<sub>3</sub>C<sub>2</sub>-NiCr coatings working under high-temperature sprayed by HVOF method. *Proceedings of the Institution of Mechanical Engineers, Part L: Journal of Materials Design and Applications* **236(12)** (2022) 2372-2383. <https://doi.org/10.1177/14644207221082237>
- [14] K. Goyal, V.P.S. Sidhu, R. Goyal, Hot Corrosion Study of High Velocity Oxyfuel (HVOF) Sprayed Coatings on Boiler Tube Steel in Actual Coal Fired Boiler, *Pakistan Journal of Scientific & Industrial Research, Series A: Physical Sciences* **61** (2018) 149-155. <https://doi.org/10.52763/PJSIR.PHYS.SCI.61.3.2018.149.155>

- [15] S. Muthu, M. Arivarasu, Investigations of hot corrosion resistance of HVOF coated Fe based superalloy A-286 in simulated gas turbine environment, *Engineering Failure Analysis* **107** (2020) 104224. <https://doi.org/10.1016/j.engfailanal.2019.104224>
- [16] M. Shi, Z. Xue, H. Liang, Z. Yan, X. Liu, S. Zhang, High velocity oxygen fuel sprayed Cr<sub>3</sub>C<sub>2</sub>-NiCr coatings against Na<sub>2</sub>SO<sub>4</sub> hot corrosion at different temperatures, *Ceramics International* **46** (2020) 23629-23635. <https://doi.org/10.1016/j.ceramint.2020.06.135>
- [17] K. Goyal, H. Singh, R. Bhatia, Current Status of Thermal Spray Coatings for High Temperature Corrosion Resistance of Boiler Steel, *Journal of Material & Metallurgical Engineering* **6** (2016) 29-35. <https://engineeringjournals.stmjournals.in/index.php/JoMME/article/view/2469>
- [18] N. Abu-warda, A. López, M. López, M. Utrilla, Ni<sub>2</sub>O<sub>3</sub> coating on T24 steel pipes by HVOF thermal spray for high temperature protection, *Surface and Coatings Technology* **381** (2020) 125133. <https://doi.org/10.1016/j.surfcoat.2019.125133>
- [19] K. Goyal, R. Goyal, Improving hot corrosion resistance of Cr<sub>3</sub>C<sub>2</sub>-20NiCr coatings with CNT reinforcements, *Surface Engineering* **36** (2019) 1200-1209. <https://doi.org/10.1080/02670844.2019.1662645>
- [20] V. P. Singh Sidhu, K. Goyal, R. Goyal, Corrosion behaviour of HVOF sprayed coatings on ASME SA213 T22 boiler steel in an actual boiler environment, *Advanced Engineering Forum* **20** (2017) 1-9. <https://doi.org/10.4028/www.scientific.net/AEF.20.1>
- [21] N. Otsuka, R. A. Rapp, Hot Corrosion of Preoxidized Ni by a Thin Fused Na<sub>2</sub>SO<sub>4</sub> Film at 900 °C, *Journal of The Electrochemical Society* **137** (1990) 46-52. <https://doi.org/10.1149/1.2086436>
- [22] G. El-Awadi, S. Abdel-Samad, E. S. Elshazly, Hot corrosion behavior of Ni based Inconel 617 and Inconel 738 superalloys, *Applied Surface Science* **378** (2016) 224-230. <https://doi.org/10.1016/j.apsusc.2016.03.181>
- [23] R. Goyal, K. Goyal, Development of CNT reinforced Al<sub>2</sub>O<sub>3</sub>-TiO<sub>2</sub> coatings for boiler tubes to improve hot corrosion resistance, *Journal of Electrochemical Science and Engineering* **12(5)** (2022) 937-945. <https://doi.org/10.5599/jese.1291>
- [24] A.C. Karaoglanli, Y. Ozgurluk, A. Gulec, D. Ozkan, G. Binal, Effect of coating degradation on the hot corrosion behavior of yttria-stabilized zirconia (YSZ) and blast furnace slag (BFS) coatings, *Surface and Coatings Technology* **473** (2023) 130000. <https://doi.org/10.1016/j.surfcoat.2023.130000>
- [25] S. Kumar, R. Bhatia, H. Singh, Hot corrosion behaviour of CNT-reinforced ZrO<sub>2</sub>-Y<sub>2</sub>O<sub>3</sub> composite coatings on boiler tube steel at 900 °C, *Anti-Corrosion Methods and Materials* **68(6)** (2021) 503-515. <https://doi.org/10.1108/ACMM-12-2020-2412>

